A NEW PARABOLIC APPROXIMATION TO

THE HELMHOLTZ EQUATION

J. Corones, R. Dougherty, and H. McMaken

Ames Laboratory USDOE and Department of Mathematics
Iowa State University
Ames, IA 50011

1. INTRODUCTION

Parabolic or forward scattering approximations are often used
to investigate acoustic or electromagnetic wave propagation in inho-
mogeneous media. Recently there has been an intensified interest in
these approximations traceable in large measure to the work of
Tappert[1] and Claerbout[2]. Tappert's work, reviewed in context in [1]
applies the Leontovich-Fock (LF) approximation with considerable
success to the study of underwater acoustics. Claerbeut has applied
these approximations in a geophysical context. The LF parabolic
approximation is very well suited to the study of sound propagation
in model oceans that have range independent sound speeds. It has
also been used to study propagation in fiber optics material,[3] as well
as in the study of laser propagation in the atmosphere.[4]

Due to these successes there have been several attempts in re-
cent years[5,6] to generalize the LF approximation so as to broaden its
range of validity. The generic physical situation to which the LF
approximation and its would-be successors models is easily specified.
A pencil of radiation, e.g., a Gaussian beam, is incident on a slab
of inhomogeneous material whose material properties are such that, at
least for a limited distance into the material, the major portion of
the incident beam propagates into the medium along the direction
defined by the initial beam axis and beam spreading is small. The
parabolic approximations are first order equations in the variable
along the initial beam axis. It should be noted that even very weak
scattering is cumulative and that for this reason a parabolic approx-
imation is not uniform in the distance into the medium; that is, even
very close to the original beam axis the approximation will break
down at a sufficient distance into the medium.

The parabolic approximations that are derived are considerably easier to integrate numerically than are the elliptic equations which they approximate, particularly in cases where complicated inhomogeneities are present or when complicated boundaries are present, e.g., the ocean and its bottom. Indeed, it is this property that makes approximations of this type attractive.

In the next section a brief discussion will be given a recently derived (improved) parabolic approximation.[5] This will be followed by the presentation and discussion of some numerical examples using this approximation.

2. DERIVATION OF THE PARABOLIC APPROXIMATION

Consider the reduced wave equation for a homogeneous medium

$$(\nabla^2 + k_o^2)\psi(\underline{x}) = 0 \tag{1}$$

The general solution to the equation is given by

$$\psi(\underline{x}) = \int A(\underline{p})\delta(k_o^2 - p^2)e^{i\underline{p}\cdot\underline{x}} \, d^3\underline{p} \tag{2}$$

The integration over p_1 can be done to yield

$$\psi(x) = \int \{A^+ e^{i(k_o^2 - R^2)^{1/2}x_1} + A^- e^{-i(k_o^2 - R^2)^{1/2}x_1}\} e^{i\underline{R}\cdot\underline{x}_\perp} d^2\underline{R} \tag{3}$$

where $\underline{R} = (p_2, p_3)$, $R = |\underline{R}|$, $x_\perp = (x_2, x_3)$ and the arguments of $A^\pm$ have been suppressed. Clearly

$$\psi^\pm(\underline{x}) = \int A^\pm e^{\pm i(k_o^2 - R^2)^{1/2}x_1} e^{i\underline{R}\cdot\underline{x}_\perp} \, d^2\underline{R} \tag{4}$$

are components of $\psi(\underline{x})$ with positive (negative) momentum in the x_1 direction. If the operators

$$P^\pm = \frac{1}{2}\{1 \pm \frac{1}{i} \frac{1}{[k_o^2 + \Delta_\perp]^{1/2}} \partial_{x_1}\} \tag{5}$$

are defined, then the $\pm$-components of $\psi(\underline{x})$ can be projected out of solutions of (1),

$$\psi^\pm(\underline{x}) = P^\pm\psi(\underline{x}), \tag{6}$$

as can easily be verified. It is not difficult to show that if $\psi(x)$ satisfies (1) and $\psi^\pm(\underline{x})$ are defined by (6) then

$$\{i \frac{\partial}{\partial x_1} \pm (k_o^2 + \Delta_\perp)^{1/2}\} \psi^\pm(\underline{x}) = 0 \tag{7}$$

This is a standard result in Fourier optics, often expressed as the transverse Fourier transform of (7).

If the medium is inhomogeneous so that the governing wave equation is

$$(\Delta^2 + k^2(\underline{x}))\psi(\underline{x}) = 0 \tag{8}$$

where $k^2(\underline{x}) = k_o^2(1+n(\underline{x}))$ it is still possible to re-express the content of (8) in terms of the variables $\psi^{\pm}(\underline{x})$ defined by (6). If the medium is weakly scattering the $\pm$-components will continue to be good approximations to the physical fields with positive and negative momentum in the x_1 direction. However, they will be coupled because of the inhomogeneity. Using the notation $S=(k_o^2+\Delta_{\perp})^{1/2}$, $S(\underline{x})=(k^2(\underline{x})+\Delta_{\perp})^{1/2}$ the wave equation (8) can be re-expressed in terms of $\psi^{\pm}(\underline{x})$ by the pair of equations

$$\left\{2i\frac{\partial}{\partial x_1} + S^{-1}S^2(\underline{x})+S\right\}\psi^+(\underline{x}) = -S^{-1}\left\{k_o^2 n(\underline{x})\psi(\underline{x})\right\}$$

$$\tag{9}$$

$$\left\{2i\frac{\partial}{\partial x_1} + S^{-1}S^2(\underline{x})+S\right\}\psi^+(\underline{x}) = -S^{-1}\left\{k_o^2 n(\underline{x})\psi(\underline{x})\right\} .$$

If it is assumed that the medium is weakly scattering so that the reflections terms (the right hand sides of (9)) can be neglected then the approximation provided by (9) for forward propagating waves is

$$\frac{\partial\psi^+(\underline{x})}{\partial x_1} = iS\psi^+(\underline{x}) + \left(\frac{k_o^2}{2}\right)S^{-1}n(\underline{x})\psi^+(\underline{x}) . \tag{10}$$

It should be noted that if this general scheme is followed but the projection operators in (5) are approximated by projectors that are valid only to leading order in R/k_o^2 the parabolic approximation derived is the Leontovich-Fock approximation.[5] Further, if the formal projector $P(\underline{x})$ is defined by

$$P^{\pm}(\underline{x}) = \frac{1}{2}\left\{1 \pm \frac{1}{iS(\underline{x})}\partial x_1\right\} \tag{11}$$

the result of Tappert[1] is recovered. The results of this section were originally derived in [5] and rederived elsewhere.[6] Related equations have also be treated.[7]

In the next section the numerical method used to integrate (10) is sketched.

3. NUMERICAL APPROACH

Equation (10) is integrated in two dimensions so that $\Delta_{\perp} = \frac{\partial^2}{\partial x_2^2}$ subject to the "initial" condition $\psi^+(x_1,0) = u(x)$ and

the boundary conditions $u(o,x_2) = u(x,max,x_2) = 0$. The latter conditions are imposed for computational convenience. The calculations are typically performed using a beam incident on a target or inhomogeneous region and are terminated before any portion of the beam hits the transverse boundary. The boundary conditions of course yield spurious reflections back into the computational grid.

To integrate (10) efficiently it is useful to first define

$$\psi(\underline{x}) \text{ by } \psi^+(\underline{x}) = e^{ix_1 S}\psi(\underline{x}) \qquad\qquad (12)$$

It easily follows that

$$\frac{\partial\psi(\underline{x})}{\partial x_1} = \frac{ik_o^2}{2} S^{-1}e^{-ix_1 S}n(\underline{x})e^{ix_1 S}\psi(\underline{x}) \qquad\qquad (13)$$

$$\equiv F(x_1, x_2, \psi)$$

The initial/boundary conditions on $\psi(\underline{x})$ follow from those on $\psi^+(\underline{x})$ and are

$$\psi(x_1, 0) = u_o(x_1)$$
$$\qquad\qquad\qquad\qquad\qquad\qquad\qquad (14)$$
$$\psi(0, x_2) = \psi(x_1\,max, x_2) = 0$$

The equation (13) is first discretized taking into account the transverse boundary conditions, in this case by using finite Fourier sine transforms (FFST). The resulting set of o.d.e.s are then integrated using a fourth order Runge-Kutta method. The discretization of (13) in the transverse variable is done by performing the following steps:

a) For any fixed $x_1 \geqslant 0$ evaluate $\psi(x_1, x_2)$ at $N = 2^m$ equally spaced points in the transverse direction;
b) perform a FFST and multiply by the FFST of $e^{ix_1 S}$;
c) perform an inverse FFST and multiply by $n(x_1, \cdot)$;
d) perform a FFST and multiply by the FFST of $\frac{1}{2k_o^2} S^{-1}e^{ix_1 S}$;
e) perform an inverse FFST.

This sequence of steps yields the discretized form of $F(x_1, x_2, \psi)$. The resulting equations are then integrated in x_1 to obtain the forward going field.

In each of the following figures the vertical axis is the x axis running from x=0 to x-1 at the top. The horizontal axis is the z axis running left to right from 0 to z_{max}. The quantity z_{max} is 1 for Figs. 1 to 3 and 0.5 for Figs. 4 to 6. The wave number has been normalized so that $k_o=210.1$. The incident field is Gaussian of the following form:

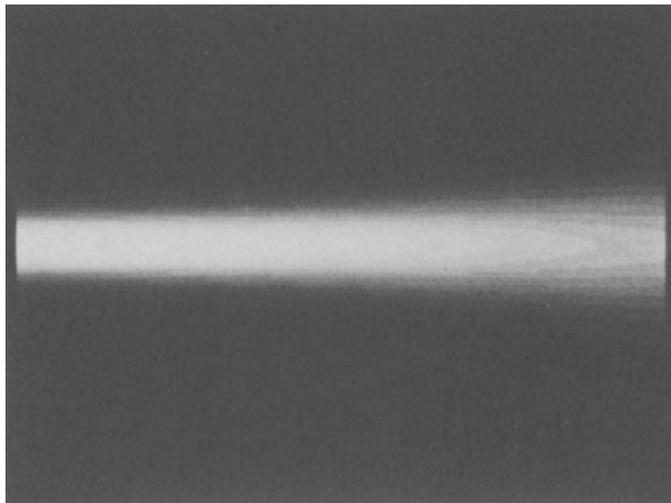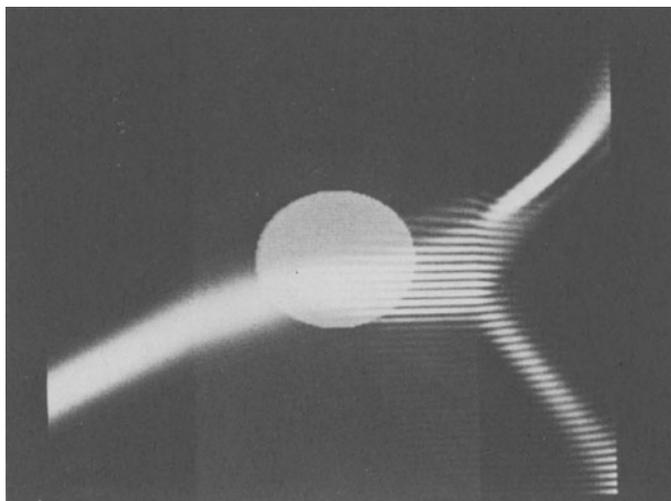$$u_{inc}(x,0) = \exp[-(x-x_o)^2/\sigma_o^2 + ik_o x \sin\alpha]$$

Figure 1

Figure 2

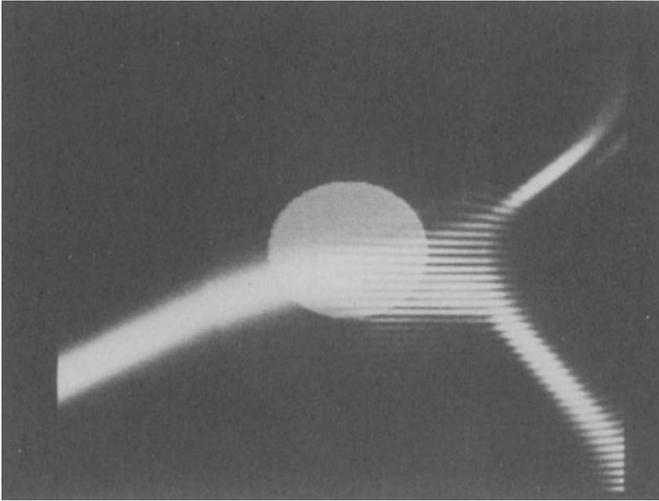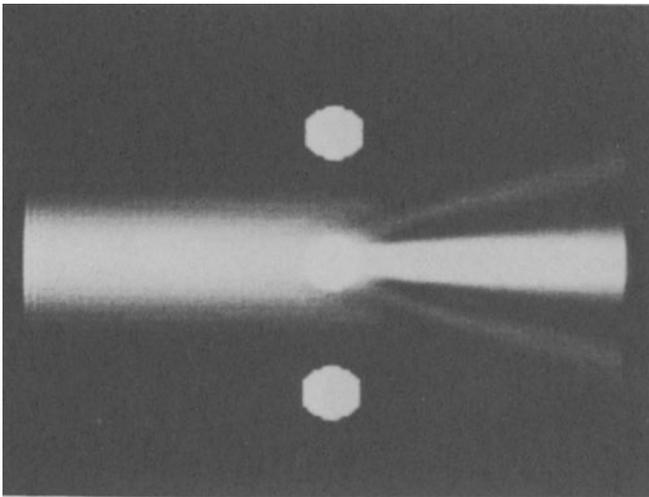Figure 3

Figure 4

The quantity x_0 is 0.5 for Figs. 1,4-6 and is 0.23 for Figs. 2 and 3. The angle α is 0° for Figs. 1, 4-6 and 30° otherwise. The quantity σ_0 is 0.07 for all figures.

In Fig. 1 we have the field present in the absence of any scatterers. In Fig. 2 $k(x,z)$ is given by

$$k(x,z) = k_0 \left[1 + .5 \exp(-(r/.14)^2) + .5H(z-.25)H(.75-z) \right]$$

where $r^2 = (x-.5)^2 + (z-.5)^2$.

As the beam passes through the interface it is refracted. As it continues toward the Gaussian bump, part of the beam is refracted, while part is reflected. As the beam passes through the trailing interface, it is again refracted. We note that the interference pattern observed near x=0, z=1 is caused by the interaction of the field with the artificial reflections due to the horizontal boundaries. In Fig. 3 we changed the leading interface from planar to curvilinear. The equation of the interface is given by

$$z = .25 + (x-.5)^2.$$

We again note the same qualitative behavior as in Fig. 2.

In Figs. 4-6, we illuminate multiple targets. Each target is a Gaussian bump of the form

$$k_j = .5 * \exp[-r_j^2/.0009]$$

where

$$r_j^2 = (x-x_j)^2 + (z-z_j)^2$$

and

$$k(x,z) = k_0(1 + \sum_{j=1}^{3} K_j).$$

In Fig. 4, the incident beam illuminates three targets at the locations

$$(x_1,z_1) = (.375, .25)$$
$$(x_2,z_2) = (.5, .25)$$
$$(x_3,z_3) = (.625, .25)$$

We note that the bumps act like a diffraction grating. We particularly note that the center bump focuses the Gaussian beam.
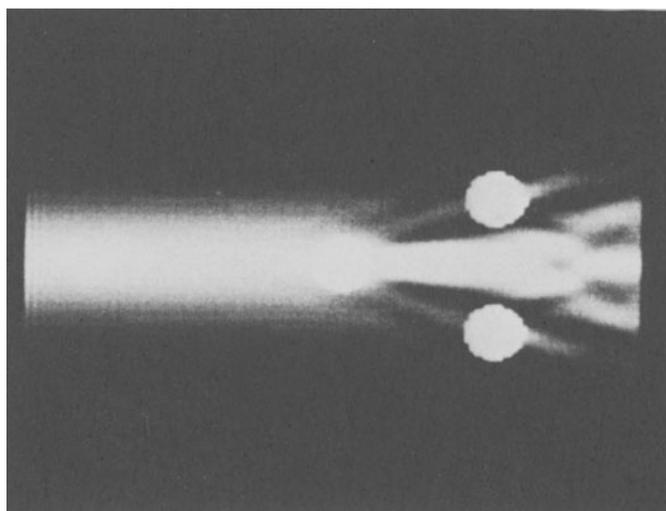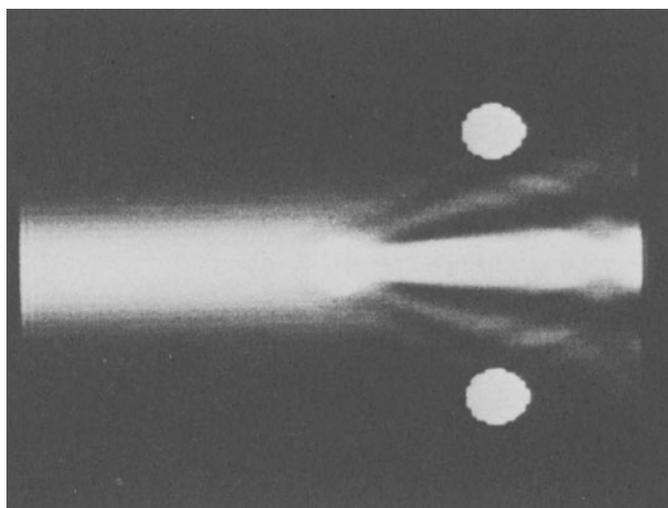
Figure 5

Figure 6

In Fig. 5, the targets are located at

$$(x_1, z_1) = (..375, .375), (x_2, z_2) = (.5, .25),$$
$$(x_3, z_3) = (.625, .375)$$

In Fig. 6, the targets are located at

$$(x_1, z_1) = (.4375, .375), (x_2, z_2) = (.5, .25),$$
$$(x_3, z_3) = (.5625, .375)$$

In this case, the trailing two targets act as a diffraction grating for the focused beam of the leading target as well as focusing side branches of the main beam. All of the above phenomena are as would be expected if one had the full solution to the Helmholtz equation.

These preliminary numerical results show that the parabolic approximation investigated here captures the correct full wave behavior of the Helmholtz equation for the targets and boundary conditions under study. A fuller qualitative investigation of the equation will be presented elsewhere.

ACKNOWLEDGEMENTS

REFERENCES

1. F. D. Tappert, The parabolic approximation method, in: "Wave Propagation and Underwater Acoustics", J. B. Keller and J. S. Papadakis, Eds., Springer-Verlag, Heidelberg (1977).
2. J. F. Claerbout, "Fundamentals of Geophysical Data Processing," McGraw-Hill Book Co., Inc., New York (1976).
3. M. D. Feit and J. A. Fleck, Jr., Calculations of dispersion in graded-index multimode fibers by a propagating beam method, Applied Optics 18:2843-51 (August 1979).
4. W. G. Tam, Split-step Fourier-transform analysis for laser-pulse propagation in particulate media, J. Opt. Soc. Am. 72:1311-1316 (1982).
5. J. P. Corones and R. J. Krueger, Higher-order parabolic approximations to time-independent wave equations, J. Math. Physics 24:2301 (1983).
6. M. E. Davison, A general approach to splitting and invariant imbedding for linear wave equations, to appear in J. Math. Anal. Appl.
7. L. Fishman and J. J. McCoy, Derivation and application of extended parabolic wave theories, to appear in J. Math. Phys.